Check for updates



www.chemsuschem.org

# Oxidative Conversion of Polyethylene Towards Di-Carboxylic Acids: A Multi-Analytical Approach

Tom J. Smak, [a] Peter de Peinder, [a] Jan C. Van der Waal, [b] Rinke Altink, [b] Ina Vollmer, \*[a] and Bert M. Weckhuysen\*[a]

To reduce the pressure on the environment created by the increasing amount of plastic waste, the need to develop suitable plastic recycling methods has become more evident. However, the chemical recycling toolbox for polyethylene (PE), the most abundant type of plastic waste, remains underdeveloped. In this work, analytical methods were developed to explore the possibility to oxidatively convert PE into dicarboxylic acids as reaction products. A multi-analytical approach including gas chromatography-mass spectrometry, gas chromatography-flame ionization detection, several (2D) nuclear magnetic resonance methods as well as in-situ transmission infrared spectroscopy was used. This led to a thorough

qualitative and quantitative analysis on the product mixture, which extends and clarifies the existing literature. Without a catalyst (thermally) already up to 7 mol% di-carboxylic acids can be formed. Furthermore, it was found that the majority of the oxidized functionalities are carboxylic acids, (methyl) ketones,  $\gamma$ -lactones,  $\gamma$ -ketones and esters. An intra-molecular hydrogen shift seemed key in the cleavage step and the formation of late-stage side products. In addition, crosslinking reactions due to esterification reactions seem to limit the dicarboxylic acid yield. Therefore, these two handles can be taken into account to study and design similar (catalytic) systems for the oxidative conversion of plastic waste.

#### Introduction

Plastic-based products have become an integral part of our daily lives, but unfortunately the extensive use of plastics has resulted in an enormous amount of plastic waste, even leading to the formation of micro- and nanoplastics, which may end up in the environment and our food chain. It is estimated that only 2% of the produced plastics is recycled globally, while 32% leaks into the environment with all its negative consequences. To limit the environmental impact of plastics, the degree of recycling must be drastically increased. [1] The currently applied recycling pathways for polyolefin (polyethylene (PE) and polypropylene (PP)) waste are mostly mechanical, but this is usually accompanied by degraded product properties. [2,3] As a result, mechanical recycling can only exist in the presence of another outlet of degraded product. For chemical recycling, degraded polyolefins are in most cases still a good feedstock

and therefore, it is of great importance that chemical recycling pathways are developed in such a way that product properties can be retained.[4] However, these new technologies are still competing with the existing fossil-based technologies, leading to cheap monomers. This problem could be possibly circumvented by e.g., oxidation towards di-carboxylic acids, where the economic value of the reaction products could be increased. In a few literature precedents, it has been shown that PE can be converted into high-value di-carboxylic acids, such as succinic and adipic acid, which have a significantly higher value compared to mechanically recycled PE, [5,6] as well as ethylene as a starting molecule. In addition to the pure monomers, a dicarboxylic acid mixture is of interest for applications, such as solvents (e.g. dibasic esters of succinic, glutaric and adipic acid are a coproduct of adipic acid manufacturing)[7] and plasticizers.[8]

Although the aerobic oxidation of PE is studied for decades, [9-11] not so much is known about the exact reaction pathways transforming PE into di-carboxylic acids. Predominantly, because the research in the past focused on preventing oxidation instead of producing products.[12,13] The majority of the reported examples focused on recycling, involve the use of  $\mbox{HNO}_3$  as oxidant.  $\mbox{\sc [14-16]}$  Ideally, the use of  $\mbox{\sc HNO}_3$  as oxidant is avoided and a greener oxidant, such as O2 is used and to avoid N<sub>2</sub>O emissions. Sen et al. have reported a non-catalytic system for the oxidation of several common polymers with O2 and NO as an additive.[17] Although the addition of NO seemed to play an important role in the reaction, it did not end up in the final product mixture. A catalytic example with O<sub>2</sub> as the oxidant was reported by Partenheimer. [18,19] He has performed experiments under similar conditions as known for industrial p-xylene oxidation with a homogeneous Co/Mn/Br catalyst. It is interesting to note that both Sen et al. and Partenheimer reported total

Debye Institute for Nanomaterials Science and Institute for Sustainable and Circular Chemistry

Utrecht University

Universiteitsweg 99, 3584 CG Utrecht (The Netherlands)

E-mail: i.vollmer@uu.nl

b.m.weckhuysen@uu.nl

[b] Dr. J. C. Van der Waal, R. Altink TNO, Brightsite Urmonderbaan 22, 6167 RD Geleen (The Netherlands)

Supporting information for this article is available on the WWW under

https://doi.org/10.1002/cssc.202301198

© 2023 The Authors. ChemSusChem published by Wiley-VCH GmbH. This is an open access article under the terms of the Creative Commons Attribution License, which permits use, distribution and reproduction in any medium, provided the original work is properly cited.

<sup>[</sup>a] T. J. Smak, Dr. P. de Peinder, Dr. I. Vollmer, Prof. Dr. B. M. Weckhuysen Inorganic Chemistry and Catalysis group,

4, 7, Downloaded from https://chemistry-europe.onlinelibrary.wiley.com/doi/10.1002/cssc.202301198 by Cochrane Netherlands, Wiley Online Library on [04/06/2024]. See the Terms and Conditions (https://onlinelibrary.wiley.com/rems-and-conditions) on Wiley Online Library for rules of use; OA articles as governed by the applicable Cerative Commons Licensea

yields of succinic, glutaric, adipic and pimelic acid up to around 40 mol %. [17,18]

Nowadays, with the increasing urge for new and better plastic recycling methods, it is important to get a deeper understanding of the thermo-oxidative conversion of PE. For aerobic oxidation reactions it is known that it is challenging to control the selectivity and that thermal oxidation events can play a significant role in the final product distribution. In this work, we investigate the non-catalytic conversion of PE into various carboxylic acid products using synthetic air as the oxidant. The reaction products obtained from the thermal oxidation were thoroughly studied with combined gas chromatography-mass spectrometry (GC-MS), gas chromatographyflame ionization detection (GC-FID) and several (2D) nuclear magnetic resonance (NMR) methods. Furthermore, the reaction process was followed by in-situ infrared (IR) spectroscopy. The combination of these analytical approaches yielded mechanistic insights and provided new handles to study similar (catalytic) systems for the conversion of PE into oxidation products, such as di-carboxylic acids.

## **Results and Discussion**

The thermo-oxidative conversion of PE into carboxylic acids was performed in batch in a Parr autoclave. The effect of the reaction parameters, namely temperature, time, and pressure, on the product distribution was studied with three different analytical approaches, namely GC-MS/GC-FID, (2D—) NMR spectroscopy as well as *in-situ* IR spectroscopy. The combination of these analytical methods provided not only new insights on the depolymerization mechanisms of PE during its thermal oxidation process, but also in the experimental parameters steering the reaction product portfolio.

# **Gas Chromatography Data and Related Product Analysis**

An initial screening of several polyethylene materials was performed (e.g., low Mw LDPE, LDPE, HDPE and HDPE waste), which were tested in mild oxidation and their product composition analyzed with GC-MS/GC-FID (SI, section 3). It was found that di-carboxylic acid yields were the highest for low Mw LDPE (~7 mol%), followed by LDPE/HDPE (~5.5 mol%) and the lowest yield was obtained for HDPE waste (~4.0 mol%). Further, a similar selectivity was observed and the main side products were observed for all polymers in a similar ratio, although low Mw LDPE shows a slightly higher selectivity to unidentified products. Because our aim is to get insights in the thermal oxidation processes in PE and develop and connect new analytical methods, we decided to select a LDPE type with a relatively low molecular weight of 4000 g/mol for this study. This choice leads to an improvement in data quality, especially for in-situ transmission-IR.

It is found that when the PE material under study was heated at relatively mild conditions under pressurized synthetic air (i.e., 130 °C, 16 h and 30 bar  $O_2/N_2$  (20/80)), it is converted into a broad range of smaller aliphatic oxidized products, as shown in Figure 1. Depending on how harsh the experimental conditions were chosen, visual inspection of the product mixtures yields an image varying from an unreacted colorless solid, to a yellow/orange gel to a brown solid. Details on this analysis can be found in the supporting information (SI, section 2). To enable good quantitative GC analysis, the carboxylic acids were fully converted to their methyl ester analogues<sup>[20]</sup> and product mixtures were analyzed using a total ion chromatogram (TIC) and flame ionization detector (FID) simultaneously. In most experiments, the complete product mixture (i.e., 125-225 mg out from 200 mg starting material) was soluble, but in some experiments, the solids formed needed to be removed by filtration. A representative example (130°C, 30 bar, 16 h) of a GC-FID chromatogram is shown in Figure 1a, which clearly shows that there are multiple repeating patterns in the

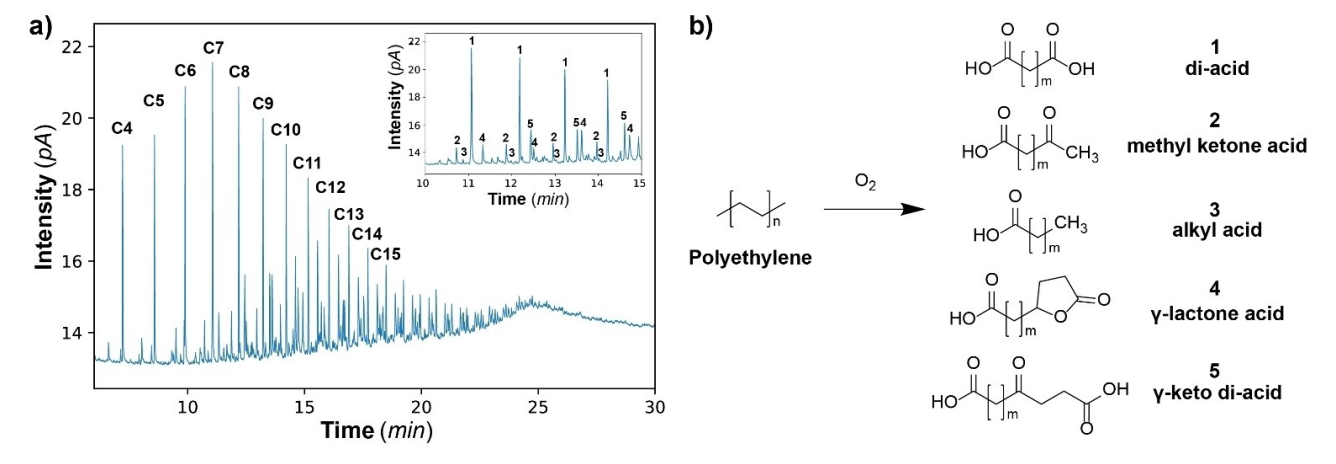


Figure 1. a) Example of a typical Gas Chromatography-Flame Ionization Detection (GC-FID) plot of the product mixture obtained from the thermal oxidation of polyethylene (PE) at 130 °C and 30 bar synthetic air for 16 h (Figure 2 and Table S1, entry 2). The figure clearly illustrates the pattern in product distribution for each carbon number. The insert shows a zoom in of the repeating patterns observed in GC-FID. b) The five major product groups making up this pattern for each chain length.

Chemistry Europe European Chemical Societies Publishing

obtained product mixture. Another set of representative examples can be found in the SI (Figure S2). Subsequently, each GC peak is assigned based on their mass spectrum (MS) and it is found that the product series with the highest intensity can be ascribed to linear di-carboxylic acids (1). The other reaction products that can be identified are carboxylic acids with a variation in the other end group functionalization (Figure 1b). Four additional chain-end functional groups are found to appear in relatively high abundance, namely methyl ketone (2), alkyl (3) (i.e., fully saturated aliphatic chain),  $\gamma$ -lactone (4) and  $\gamma$ keto carboxylic acid (5). Thereafter, with the help of an internal standard, the yield for all individual reaction products were calculated and they were grouped based on their chemical characteristics (i.e., functional group and carbon number). The yields are shown in Figure 2 and are defined as the molar percentage of carbon from the polymer that ends up in the products (an example calculation in the SI (Section 2)). Reaction conditions were optimized for the oxidative conversion of PE and the results are summarized in Figure 2. From the product distributions it was evident that in nearly each experiment dicarboxylic acids (1) are the main product, followed by carboxylic acids where the second end group is a methyl ketone (2), alkyl (3),  $\gamma$ -lactone (4) or  $\gamma$ -keto carboxylic acid (5).

In each experiment roughly two thirds of the peaks, accounting for one third of the total integral under the entire chromatogram, cannot be ascribed to specific chemical structures. In general, it was not possible to obtain a MS spectrum of sufficient quality for these species as they were present in very low amounts leading to a low signal-to-noise ratio. However, it is likely that a noticeable amount of the unidentified compounds have similar chemical characteristics as the identifiable products. Furthermore, most of the unidentified species appear at higher retention times, indicating these are larger fragments (e.g., C > 15). It is not surprising that the number of side product increases with carbon number, since the number of possibilities for combinations of functional groups increases exponentially. Using the optimized product analysis method, the reaction time was screened first (Figure 2a/d), keeping the temperature and pressure fixed at 130°C and 30 bar respectively. It is found that the conversion increases significantly from 8 to 16 h, but that doubling the time to 32 h does not lead to a further increase in yield. In fact, it seems that a longer reaction time leads to recombination of the existing products (Figure 2d), since the fraction of C23+ products has increased significantly; this crosslinking will be discussed in more detail later on. The relatively low yield at 8 h could be due to an induction period, which is often observed for auto-oxidation reactions. [21] Interestingly, the 8 h reaction (Figure 2a) is the only condition, where di-carboxylic acids (1) are not the main product, but larger amounts of carboxylic acids with methyl ketone (2) and alkyl (3) chain end groups were observed. The relative contribution of product 2 and 3 is also higher at lower temperature (Figure 2b), at which the reaction presumably proceeds more slowly. A potential explanation for the relatively large amount of alkyl acids at early-stage in the reaction, is that the cleavage starts near the chain ends of the polymer. On the other hand, side reactions such as decarboxylation are deemed unlikely to cause the formation of alkyl end groups at these mild conditions as decarboxylation is expected to increase at harsher conditions. This is further supported by a control experiment in which azaleic acid (HOOC(CH<sub>2</sub>)<sub>7</sub>COOH) is oxidized at 130 °C for 16 h (Figure S3). In this case, the decarboxylated product is not observed. The other functionality with a relatively high concentration at milder conditions was the methyl ketone,

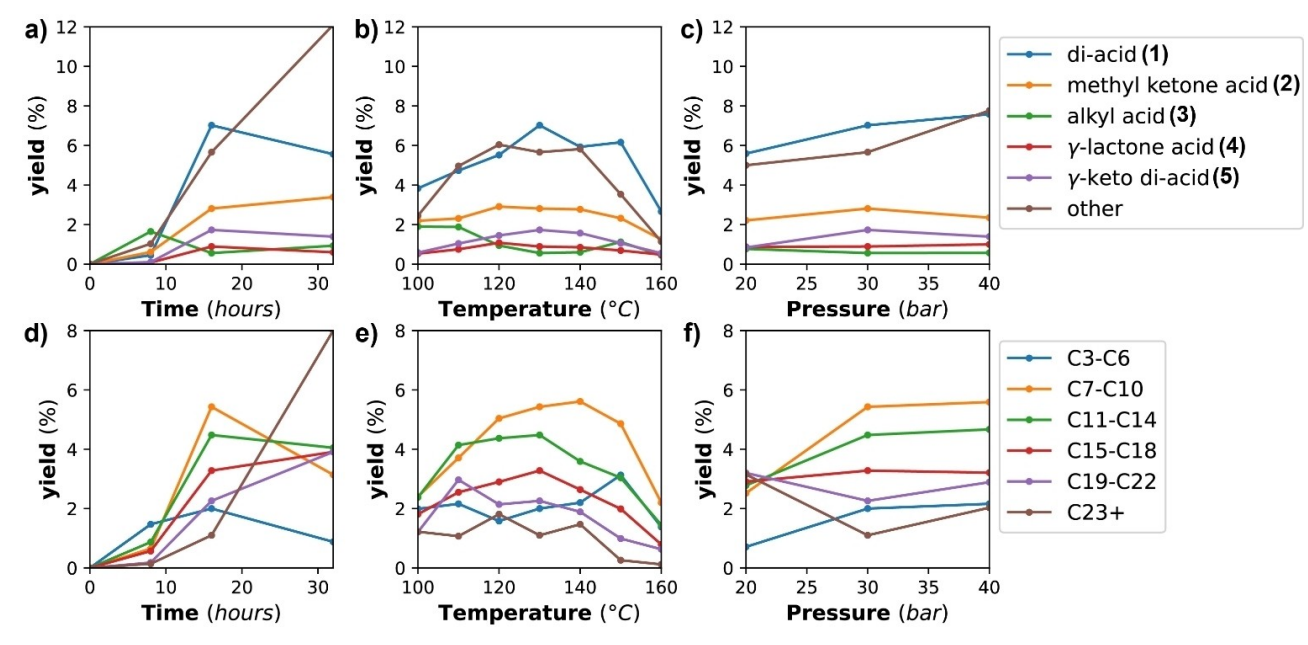


Figure 2. The yields obtained from the reaction condition screening for the thermal oxidation of polyethylene (PE). The top row shows how the variation of product distribution while the bottom row shows the variation of chain length distribution time (a, d), temperature (b, e) and pressure (c, f). The parameters were varied systematically, while keeping the other parameters fixed at the standard reaction temperature of 130 °C, pressure of 30 bar and reaction time of 16 h. All experiments were performed under pressurized synthetic air, O<sub>2</sub>/N<sub>2</sub> (20/80).



which is a commonly formed cleavage product in auto-oxidation processes. It is a decomposition product of an intermediate that is formed from an intra-molecular hydrogen abstraction by peroxyl radical, [22,23] of which the formation mechanisms will be discussed in more detail later on.

Screening the effect of reaction temperature, while keeping the time and pressure fixed at 16 h and 30 bar respectively, it is found that comparable results are obtained for the temperature range between 110–150 °C (Figure 2b/e). Increasing the temperature beyond 150°C, leads to a charred over-oxidized reaction mixture, while a decrease in temperature leads to almost no oxidation. At last, the pressure was varied, while temperature and reaction time were fixed at 130 °C and 16 h respectively (Figure 2c/f). An increase in pressure to 40 bar leads to an increased di-carboxylic acid yield up to ~7.5 %, while a decrease in pressure to 20 bar leads to small drop in the yield to ~5.5 %. In addition to the analysis based on functional groups, the average chain length of the products observed with GC was compared. When temperature and pressure were varied, it was found that there is no clear trend in carbon number (Figure 2e/ f). Most of the experiments gave a similar result. The only significant deviations in carbon number are observed at higher temperature at or above 150°C (Figure 2e), which results in a decrease in chain length.

For each experiment, the quantity of carbon that was observed with GC-FID was significantly less than expected. The incorporation of oxygen leads to a mass increase of the final product. Starting from 200 mg we recovered about 125-225 mg oxidized product depending on the experimental conditions. However, with GC-FID, we could quantify approximately 30-40 mg carbon. It seems that the missing mass appears as an increase in background towards higher retention times (Figure S4). This baseline increase can be explained by recombination of products and crosslinking reactions, resulting in many different products that appear at higher retention times. Due to the large number of different products formed, there is a significant overlap between peaks. In addition, the concentration of each individual product is low. This combined with the already low overall product to solvent ratio makes it hard to determine a proper baseline subtraction method. Therefore, NMR and IR spectroscopy were used as complimentary analytical techniques to study the bulk product mixtures obtained during the oxidation experiments of PE. These results will be discussed in the subsequent sections.

# **Nuclear Magnetic Resonance Spectroscopy and Related Product Analysis**

NMR is a powerful tool for resolving chemicals structures and to detect even small amounts of oxidized functionalities in PE. However, is not trivial to obtain spectra of sufficient quality, since measurements need to be performed in 1,1,2,2-tetrachloroethane or 1,2,4-trichloro benzene above 100 °C to dissolve the material. However, it was found that highly oxidized polyethylene is soluble in acetone, enabling analysis at room temperature. In addition to <sup>1</sup>H and <sup>13</sup>C NMR, three

different types of 2D NMR experiments were performed on the whole product mixture (120°C, 16 h, 30 bar O<sub>2</sub>/N<sub>2</sub>), namely, heteronuclear single quantum coherence (HSQC), heteronuclear multiple bond coherence (HMBC) and <sup>1</sup>H – <sup>1</sup>H total correlation spectroscopy (TOCSY). Figure 3a and b show the <sup>1</sup>H and <sup>13</sup>C NMR spectrum of oxidized PE, respectively. As expected from the GC data, a first look at both NMR spectra shows that the product mixture is complex in nature and consists of a wide variety of different reaction products. In the <sup>1</sup>H NMR spectrum, the highest intensity is observed in the aliphatic region, with the -CH<sub>2</sub>- signal at 1.08 – 1.69 ppm and the -CH<sub>3</sub> peak at 0.74-1.06 ppm. The region between 1.9 and 2.8 ppm can be ascribed to protons at the  $\alpha$ -position next to a carbonyl. The region from 3.5-5.0 ppm is indicative for C-O species and the weak signals at 8.1 ppm are indicative for peroxide species.  $^{\rm [26]}$  The  $^{\rm 13}{\rm C}$  NMR spectrum is shown in Figure 3b and a large variety of oxidized species was observed. The spectrum can be roughly divided into different areas, namely, aliphatic (15-50 ppm), C-O (60-85 ppm) and carbonyl (170–180 ppm, acid, ester,  $\gamma$ -lactone and 200–210 ppm, ketone). Zoom-ins for all NMR data of all relevant spectral regions can be found in the SI (section 7). Using the coupling patterns in the three different 2D experiments, it was possible to obtain a nearly complete interpretation of the <sup>1</sup>H and <sup>13</sup>C spectra. All correlations used for the assignments are tabulated in the SI (section 5).

Firstly, HSQC NMR measurements were performed to get insights into which H and C atoms are coupled. This experiment is especially interesting for the characterization of functional groups containing a C-O single bond (e.g., alcohol, ester, and  $\gamma$ -lactone); a zoom-in of this region is shown in Figure 3c. The HSQC NMR spectrum enabled the visualization of secondary alcohols, which are only observed in small quantities at 3.6 ppm in <sup>1</sup>H NMR and 70.7 ppm in <sup>13</sup>C NMR.<sup>[27]</sup> Furthermore, it is found that ester groups were present in significant quantities and the HSQC NMR experiment made it possible to distinguish between two types of esters, originating from a primary and secondary alcohol respectively. In addition, the HSQC NMR spectrum confirmed the presence of  $\gamma$ -lactones as a coupling was observed at 4.5 ppm in <sup>1</sup>H NMR and 80.5 ppm in <sup>13</sup>C NMR. Subsequently, with TOCSY NMR (Figure S24) this assignment is confirmed, since it is observed that this characteristic  $\gamma$ -lactone proton couples at the expected locations of 1.7, 1.9 and 2.4 ppm. Figure 3d shows the full spectral range of the HMBC NMR experiment, which visualizes the coupling between <sup>1</sup>H–<sup>13</sup>C over 2-4 bonds. This experiment was used to study the chemical surroundings of carbonyl groups. In the carbonyl region, we assign the carboxylic acid (174.3 ppm),[24] primary ester (172.8 ppm), [28] secondary ester (172.6 ppm), [28]  $\gamma$ -lactone (176.5),  $^{[29]}$  methyl ketone (205.4 ppm),  $^{[30]}$   $\gamma\text{-keto}$  acid (174.7 and 209.1 ppm)<sup>[24,31]</sup> and ketone (209.7 ppm).<sup>[27]</sup> In addition to the main components, there are a lot of minor components, of which the exact structure could not be resolved. A large fraction of this variation can be explained by the variation in chain length, as observed with GC, which gives small changes in the observed chemical shift. One of the minor components that was detected was identified as the furanone structure, with its characteristic doublet at 5.8 and the second peak at 7.0 ppm in

4,7, Downloaded from https://chemistry-urope.onlinelibrary.wiley.com/doi/10.1002/cssc202301198 by Cochrane Netherlands, Wiley Online Library on [04/06/2024]. See the Terms and Conditions (https://onlinelibrary.wiley.com/terms-and-conditions) on Wiley Online Library for rules of use; OA articles are governed by the applicable Creative Commons License

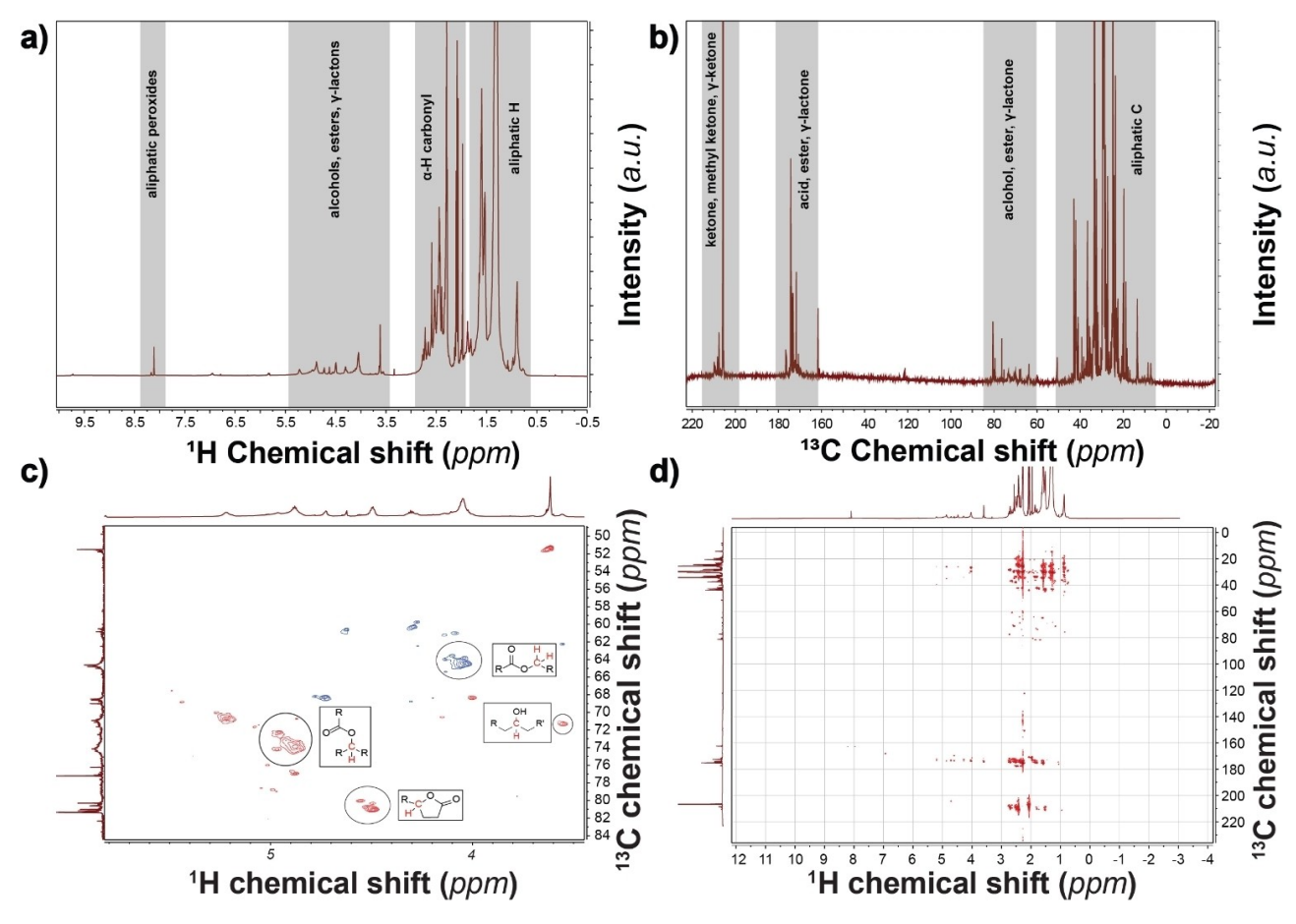


Figure 3. Nuclear Magnetic Resonance (NMR) spectra were measured on the crude reaction mixture obtained from the autoclave that was dissolved in acetone- $d_6$ . The applied conditions for sample preparation in the autoclave were 120 °C for 16 h at 30 bar synthetic air (Table S1, entry 6). An infrared (IR) spectrum of the sample can be found in the supporting information (SI), section 4. a) <sup>1</sup>H NMR spectrum b) <sup>13</sup>C NMR spectrum c) A zoom-in of the C–O single bond region HSQC of the NMR spectrum. The spectrum shows the presence of secondary alcohols, esters (primary and secondary) and γ-lactones. d) HMBC NMR spectrum of the full spectral range. The HMBC spectrum enabled assignments of all α-carbonyl protons. A table with all correlations observed resulting to the assignments are shown in the SI (section 5).

<sup>1</sup>H NMR. Furthermore, aliphatic peroxides, a key reaction intermediate in auto-oxidation reactions, were only observed in trace quantities at 8.1 ppm in <sup>1</sup>H NMR.<sup>[26]</sup>

Using the information obtained from the HSQC, HMBC and TOCSY NMR experiments, it was possible to assign all major species including all species observed with GC (carboxylic acid, methyl ketone,  $\gamma$ -ketone and  $\gamma$ -lactone and alkyl chain ends). Subsequently, with the use of the integrals obtained from the <sup>1</sup>H NMR spectrum, relative contributions of each functional group were calculated for the sample oxidized at 120°C and one that was oxidized at 140 °C (SI, section 6 for the procedure). An overview of the estimated relative contributions in NMR are shown in Figure 4. It was found that for the sample oxidized at 120°C, carboxylic acids are the main product with approximately 58%. The three different ketone species, (regular) ketone, methyl ketone and  $\gamma$ -ketone, made up 7.8, 12.4 and 3.0%, respectively. In contrast to GC, it was possible with NMR to visualize two types of esters, the primary and secondary ester contributed with respectively 7.2 and 7.0% significantly to the total carbonyl content. When the oxidation temperature was increased to 140 °C, a decrease in carbonyl content was observed and the relative product distribution changed significantly.

Although the relative concentration of carboxylic acid, methyl ketone,  $\gamma$ -ketone and  $\gamma$ -lactone stayed similar like observed with GC, the amount of both primary and secondary ester increased drastically. The increasing amount of cross-linking through ester formation provides insights about the incomplete carbon balance found with GC. The species that were not observed with GC are likely long chain products (C15 +) containing several ester functionalities.

From the integrals of the  $^1H$  NMR spectrum, it was possible to estimate the average chain length, by taking number of oxidized groups and chain ends (acid, alkyl,  $\gamma$ -lactone) into account (SI, section 6). The average chain lengths for the samples oxidized at  $120\,^{\circ}\text{C}$  and  $140\,^{\circ}\text{C}$  were 16 and 25 carbons, respectively. For both samples, the estimated chain length determined with NMR was significantly higher than observed with GC-FID and GC-MS, especially for the ester rich sample. Further, it was estimated based on NMR that respectively 27 mol% ( $120\,^{\circ}\text{C}$ ) and  $32\,\text{mol}\%$  ( $140\,^{\circ}\text{C}$ ) gaseous products should have been formed. These results, support the hypothesis

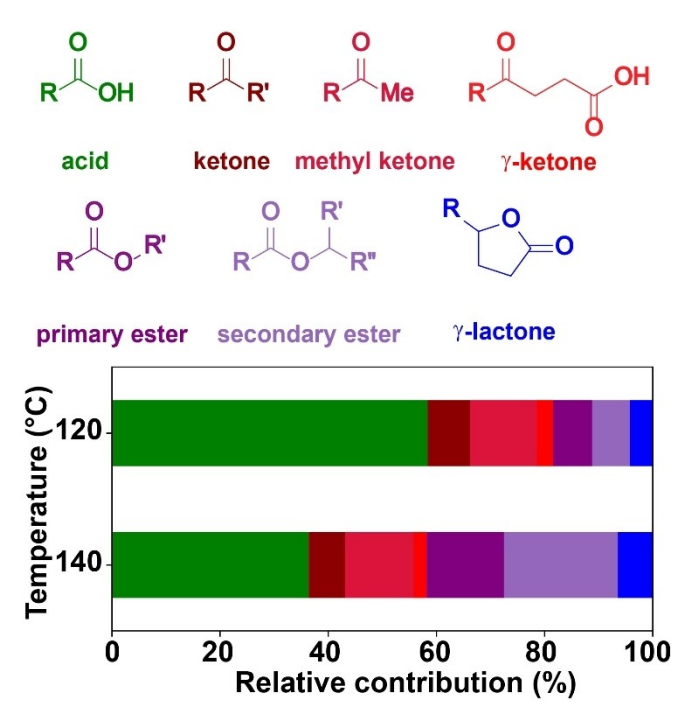


**Figure 4.** Overview of the relative carbonyl contribution determined with NMR. After the identification of all species, the relative carbonyl concentration was estimated based on the integrals obtained from the <sup>1</sup>H spectrum (procedure in SI, section 6). Nuclear Magnetic Resonance (NMR) spectra were measured on the crude reaction mixture obtained from the autoclave that was dissolved in acetone-d<sub>6</sub>. The applied conditions for sample preparation in the autoclave were 120 °C or 140 °C for 16 h at 30 bar synthetic air.

that the mismatch between product mass quantified with GC-FID and GC-MS and weighted product is likely due to larger molecules that appear as an increase in background at higher retention times.

## In-situ IR Spectroscopy and Related Product Analysis

In the final part of our study, in-situ transmission IR spectroscopy was used to obtain further information of the product formation as function of time. The experiments were performed at ambient pressure air at a fixed temperature of 170 °C. Since it was not possible to perform experiments under the exact same conditions as in the reactor, the in-situ IR data were validated with IR spectra of reactor samples. The IR spectra of the reactor experiments are shown in the SI (section 4) and it was found that there were only minor differences in the shape of the IR spectrum. Differences were observed in the level of oxidation, which was higher for the samples prepared in the autoclave. However, this did not result in a significant change in the shape of the IR spectrum and the peak locations were identical compared to in-situ IR spectroscopy. As a result of the higher oxidation levels, only the weak peaks ascribed to the isolated (non-hydrogen bonded) carboxylic acid disappeared for the autoclave samples. Figure 5a shows the whole spectral range of the in-situ IR spectra from the oxidation of PE as function of time. All IR spectra were normalized at the C-H<sub>2</sub> bend vibration (1460 cm<sup>-1</sup>) of polyethylene, since the sample thickness gradually decreased during the experiment. The C-H<sub>2</sub> bend vibration band was selected for normalization, since its intensity stayed fairly constant during the experiment; in addition, the use of the C-H<sub>2</sub> stretch vibrations (2800–3000 cm<sup>-1</sup>) were not suitable for normalization due to saturation effects and this spectral region was therefore neglected. In Figure 5a it can be seen that new functional groups appear as function of time (from blue to red). These different regions can be roughly assigned to three types of vibrations, namely the O-H stretch (3000-3600 cm<sup>-1</sup>), the C=O stretch (1600-1800 cm<sup>-1</sup>) and the C-O stretch (1100-1300 cm<sup>-1</sup>) region.<sup>[35]</sup> A zoom in of the carbonyl region is shown in Figure 5b and, as expected, the carbonyl region is complex and consists of multiple overlapping functional groups. As a result, interpreting this area reliably is difficult and the literature is often contradictory, while at the same time little supporting evidence for the assignments is provided. The multi-analytical approach enabled us to critically revise the existing IR literature  $^{[35-37]}$  and based on the input of GC-MS, GC-FID, multiple (2D-) NMR experiments in combination with the existing literature assignments, [35-37] the peaks were assigned as follows; associated carboxylic acid (H-bonded dimer) (1713 cm<sup>-1</sup>), ketone (1720 cm<sup>-1</sup>), ester (1739 cm<sup>-1</sup>), isolated carboxylic acid (1765 cm<sup>-1</sup>) and  $\gamma$ -lactone (1788 cm<sup>-1</sup>). [36,37] In the literature, the peak at 3550 cm<sup>-1</sup> is almost exclusively ascribed to an alkyl peroxide.[37] We propose that this vibration can be ascribed to the O-H stretch of an isolated carboxylic acid, because we observe the corresponding carbonyl (1765 cm<sup>-1</sup>).[35] Furthermore, the free O-H stretch vibration of an isolated carboxylic acid is expected to yield a sharp peak at 3550 cm<sup>-1</sup> as we observe and typically has a lower extinction coefficient (E) compared to the dimeric form, which appears as a broad peak with high intensity.[35] Although peroxides are most certainly formed, they have a low thermal stability, which makes their presence in high concentration unlikely. Our NMR spectroscopy data showed that peroxides were only present in trace quantities, making this assignment to a peroxide unlikely. At last, when we zoom in to the C-O stretch region two main peaks appear at 1170 and 1240 cm<sup>-1</sup>, which can be ascribed to the ester<sup>[30]</sup> and carboxylic acid<sup>[35]</sup> respectively.

Since, the carbonyl region is complex in nature, it is hard to discern the contributions of individual species. Therefore, time resolved information was extracted with the use of a peak fitting model (Figure 5c). Each of the functional groups found to be present in significant amounts based on the GC-MS, GC-FID and NMR spectroscopy data were modeled. Components that were present in minor quantities were excluded, since these increase the risk that the model converges to chemically unrealistic solutions. The fitted species were, carboxylic acid (isolated and associated), ester (secondary and primary), (methyl) ketone and  $\gamma$ -lactone. Subsequently, each spectrum was fitted using a Voigt function and an example of such a fit for a representative spectrum is shown in Figure 5c. Furthermore, the peak locations were fixed and restrictions were placed on the maximum full width half maximum (FWHM). The fitted areas were integrated and plotted as a function of time (Figure 5d). The fitting model describes the main features of the

4,7, Downloaded from https://chemistry-urope.onlinelibrary.wiley.com/doi/10.1002/cssc202301198 by Cochrane Netherlands, Wiley Online Library on [04/06/2024]. See the Terms and Conditions (https://onlinelibrary.wiley.com/terms-and-conditions) on Wiley Online Library for rules of use; OA articles are governed by the applicable Creative Commons License

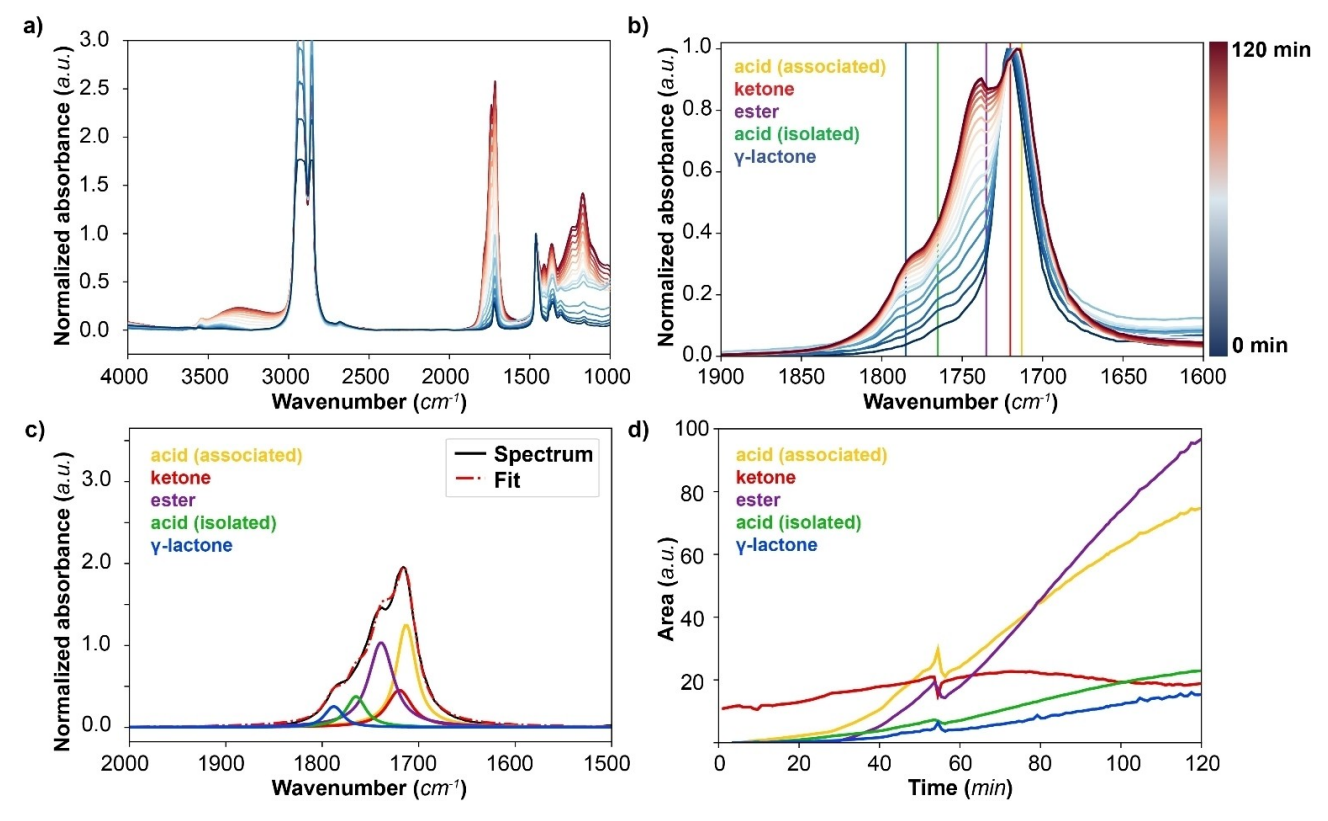


Figure 5. In-situ infrared (IR) spectra data of polyethylene (PE) oxidation. The experiments were performed at 170 °C under ambient conditions. a) Complete spectral range normalized at the C-H<sub>2</sub> bend vibration of PE (1460 cm<sup>-1</sup>). b) A zoom-in of the normalized carbonyl region, which shows the presence of multiple carbonyl species; namely, acids, esters, ketones and γ-lactone. c) A representative example of a performed curve fitting procedure applied to a spectrum (recorded after 80 min). The *in-situ* IR spectra were normalized at the C-H<sub>2</sub> bending vibration at 1460 cm<sup>-1</sup> and to the carbonyl region five different species were fitted: namely, carboxylic acid associated (1713 cm<sup>-1</sup>), ketone (1720 cm<sup>-1</sup>), ester (1739 cm<sup>-1</sup>), isolated carboxylic acid (1765 cm<sup>-1</sup>) and γ-lactone (1788 cm<sup>-1</sup>). d) The integrated fitted band areas as a function of reaction time. The discontinuity in the lines can be explained by a reorganisation of the polymer melt. More details are reported in the experimental section (SI, section 1).

system and no major systematic errors were observed; the residual intensities are plotted in Figure S26. In the IR data, from the product evolution observed over time, it can be seen that initially some ketone species were present. Then, after around 10 min carboxylic acid (both isolated and associated) species start forming and at around 30 min ester and  $\gamma$ -lactone products appear. The relative concentration of these late-stage oxidation products increases with the level of oxidation.

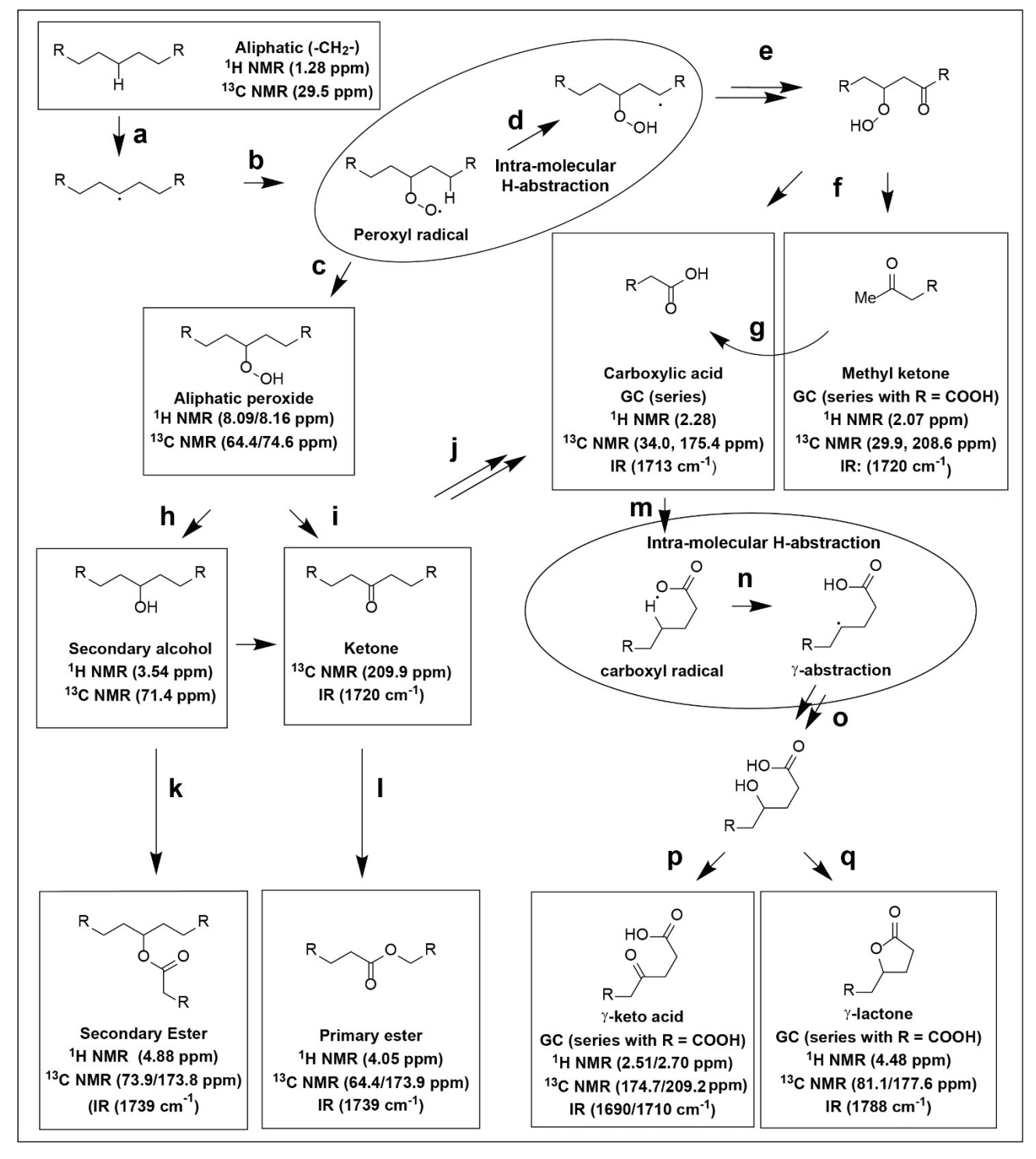
The *in-situ* IR measurements show that product formation occurs in a similar order as observed with GC and NMR experiments at 120 and 140 °C, where initially, ketones and carboxylic acids are the main product, while later in the reaction esterification reactions seem to play an important role at higher conversions.

# **Reaction Product Formation Mechanism**

Combining the information, obtained from the GC-MS, GC-FID and (2D) NMR spectroscopy measurements, allows to propose a plausible formation mechanism of the main reaction products (Scheme 1). It is well known that most steps in aerobic oxidations proceed through a radical based mechanism<sup>[36]</sup> and in Scheme 1a the initiation step in of the auto-oxidation process

is shown. Hence, the first step leads to the formation of an aliphatic radical; It is expected that a H abstraction on a tertiary carbon is preferred over an abstraction at a secondary carbon as thus initiation should be easier on a branched PE. [43] However, we observed a similar product selectivity for LDPE compared to the less branched HDPE (SI, Section 3). Subsequently, this aliphatic racial reacts with oxygen and forms a peroxyl radical, which abstracts a H radical from the surroundings, forming a peroxide, which decomposes into an alcohol or ketone (Scheme 1h/i). It is generally assumed, that all higher oxidized species originate from these species. [34]

Carboxylic acids are the most abundant reaction product, likely due to their relatively high chemical stability. For the aerobic oxidation of hydrocarbons, a large amount of literature is available, and several routes towards carboxylic acids are proposed. Considering the significant contribution of methyl ketone species especially at the beginning of the reaction, it is proposed that a significant amount of the carboxylic acids is formed through a Korcek type mechanism (Scheme 1f). The peroxyl radical formed in the early stages of the reaction abstracts a H atom from the surroundings. Given the fact that intramolecular reactions are faster than intermolecular reactions, it is no surprise that the H abstraction occurs at the  $\beta$ -carbon within the polymer chain, through a six



Scheme 1. A proposed simplified reaction scheme that correlates the main reaction products observed with GC, NMR and IR. In addition, all analytical characteristics indicated for the products that are observed. The circles highlight the intra-molecular H abstraction steps, which are important for the observed selectivity. a) Reaction initiation leading to the formation of an aliphatic radical. b) When  $O_2$  is present, the aliphatic radical will react and form a peroxyl radical. c) The peroxyl radical gets quenched by an H atom from the surrounding and forms an aliphatic peroxide. d) Kinetically it is favourable to do an intra-molecular H-abstraction at the  $\beta$ -position through a six membered ring transition state. The abundancy of the methyl ketone product suggests that this pathway is favourable. e) The formation of a radical at the  $\beta$ -position lead to oxidation at this position. f) The formed 1,3-hydroperoxyketone is known to decompose in a carboxylic acid and a methyl ketone. g) In consecutive oxidation steps, the methyl ketone can be converted to a carboxylic acid. h/i) Peroxide species are known to decompose in a secondary alcohol or ketone. j) in consecutive steps the alcohol can be oxidized to a ketone, which can be further oxidized to a carboxylic acid. k) NMR showed that large amounts of secondary esters are formed, these are formed between a condensation reaction between a carboxylic acid and a secondary alcohol. l) Since the formation of primary alcohols is highly unlikely, the formation of primary esters is presumably formed through a Baeyer-Villiger mechanism. m) A carboxyl radical can be induced by the chemical surroundings or the decomposition of a peracid.  $^{(4,2)}$  n) Similar to a peroxyl radical, it can undergo an intra-molecular H abstraction leading to a C–H abstraction at the  $\gamma$ -position, resulting in the formation of the alcohol functionality a  $\gamma$ -keto acid is formed. q) In the case of a condensation reaction a  $\gamma$ -lactone is formed.



membered ring transition state. As a result, a second oxidized group is formed at this position, yielding a thermally instable 1,3 oxidized product that decomposes into a carboxylic acid and a methyl ketone. In addition, it is proposed that a similar six membered ring transition state<sup>[40]</sup> is needed for the formation of  $\gamma$ -lactones and  $\gamma$ -keto carboxylic acids; when a carboxyl radical abstracts an H atom at the  $\gamma$ -carbon, resulting in a peroxide at the  $\gamma$ -position that decomposes into an alcohol or ketone ( $\gamma$ -keto) group respectively (Scheme 1p/q). The alcohol can undergo subsequent oxidation steps or undergo a condensation reaction that results in the observed  $\gamma$ -lactone. For this reaction pathway, a carboxyl radical needs to be present, which is known to be highly unstable and prone to decarboxylation. However, thermodynamically it is preferred to form a O-H bond over a C-H bond and it is reported that carboxyl radicals can undergo an intra-molecular hydrogen shift before decarboxylation occurs.<sup>[40]</sup> At last, step k/l of Scheme 1 show the formation of both primary and secondary esters, which were both observed in the HSQC NMR experiment. It is expected that initial oxidation events result in the formation of secondary (and tertiary) alcohol groups along the polymer chain; subsequently, these alcohols can form an ester through a condensation reaction with a carboxylic acid. [26] Primary alcohols were not expected, since the activation energy for oxidizing a CH<sub>3</sub> chain end is much higher. Therefore, it is proposed that the esters derived from a primary alcohol are predominantly formed through a Baeyer-Villiger type mechanism, which is a nonradical rearrangement of a peroxide or peracid[33] and a ketone, yielding an ester and an acid. In this case the peroxide can react directly or is converted to a peracid first.[33] This type of reactivity was observed before in the oxidation of polyketones.[34] In addition to the reactions described above, it is expected that many (competing) reaction pathways can take place. For example, the presence of aldehydes, observed in trace quantities in NMR might suggest that oxidation steps can also start by H abstraction at the  $\alpha\text{-carbon.}^{\text{[41]}}$  Furthermore, under the applied reactions conditions a lot of different reactions can occur; to name just a few examples, reactions such as decarboxylation, [34] decarbonylation, [45] condensation reactions, [32] dehydrations and many more. However, the reaction mixture is too complex to identify these pathways with sufficient certainly. Nevertheless, it can be concluded that an intra-molecular H abstraction seems to steer the selectivity towards the main reaction products observed.

# **Conclusions and Outlook**

The product mixture obtained from the thermo-oxidative conversion of polyethylene (PE) at increased conversion levels consists mainly of carboxylic acids. Additionally, ketone, methyl ketone,  $\gamma$ -lactone, primary and secondary esters and  $\gamma$ -keto acid are observed. Early-stage and short-lived products, such as peroxides and secondary alcohols, were only observed in trace amounts. These products were successfully identified and quantified with the help of GC-MS, GC-FID and several (2D) NMR spectroscopy experiments. Based on these observations

we were able to refine previous assignments proposed in the IR literature on oxidation. Furthermore, time resolved information was obtained with in-situ transmission IR and we able to confirm the GC-MS/GC-FID and (2D-) NMR findings. More specifically, it was found that initially mainly ketones were present, after which carboxylic acids form. In later stages of the reaction, the relative contribution of  $\gamma$ -lactones and esters increases significantly. Based on the combination of analytical techniques, it was proposed that an intra-molecular H-abstraction is the selectivity-determining step in the formation of all major reaction products. It was suggested that the initial step in the chain cleavage is an intra-molecular H-abstraction by a peroxyl radical through a six membered ring transition state, yielding a carboxylic acid and methyl ketone product. It is proposed that the  $\gamma$ -lactone and  $\gamma$ -keto acid form through a similar six membered ring transition state, where a carboxyl radical abstracts a hydrogen atom at the  $\gamma$ -position. As dicarboxylic acids are the high-value products, catalyst development should aim for altering the cleavage mechanism since intra-molecular H-abstraction does not necessary lead to high yields of di-carboxylic acids. In addition, we recommend to look for solutions to minimize crosslinking reactions. These solutions might be catalytic (e.g., stimulate alcohol oxidation to minimize condensation reaction) or more practical such as the use of solvents. Some preliminary in-situ transmission IR results with a catalyst material can be found in the supporting information (section 11), demonstrating the effect of the addition of e.g., Co<sub>3</sub>O<sub>4</sub> and Fe<sub>3</sub>O<sub>4</sub> materials. Further research will be focused on exploring the addition of both homogeneous and heterogeneous catalysts, as well as different solvents and oxidants.

# **Experimental Section**

#### **Chemicals and Materials**

Polyethylene (PE) was obtained as a powder from Sigma-Aldrich and was used as received. All properties mentioned are indicated by the supplier, except stated otherwise. This PE material had the following properties: mass average molar mass (Mw) = 4000 g/mol, number average molar mass (Mn) = 1700 g/mol, melting point  $(T_m) = 98$  °C as measured with differential scanning calorimetry (DSC, ref SI, section 10),  $T_m$  (supplier) = 92 °C and density ( $\rho$ ) = 0.92 g/mL. The LDPE (Lupolen 3020H) material was obtained as pellets from LyondellBasell and was used as received. The LDPE material had the following properties:  $\rho = 0.928 \text{ g/mL}$ ,  $T_m$  (DSC)= 110 °C, melt flow rate  $(190 \, ^{\circ}\text{C}/2.16 \, \text{kg}) = 2 \, \text{g}/10 \, \text{min}$ . The HDPE material was obtained as pellets from Sigma-Aldrich and was used as received. The HDPE material had the following properties:  $\rho$  = 0.952 g/mL,  $T_m$  (DSC) = 127 °C,  $T_m$  (supplier) = 125 - 140 °C, melt flow rate  $(190 \,^{\circ}\text{C}/2.16 \,\text{kg}) = 12 \,\text{g}/10 \,\text{min}$ . As HDPE waste material a Prodent toothpaste tube was selected, which was washed and cut into flakes. The HDPE waste material had the following properties:  $T_m = 125$  °C. DSC data of the used polymers is reported in the SI, section 10. The other chemicals that were used were methanol (Sigma-Aldrich, > 99.9%), n-heptane (Sigma-Aldrich > 99%), acetyl chloride (Sigma Aldrich, >99%), cyclo-octane (Sigma Aldrich, >99%), 4-heptanone (Across Organics, >98%) and acetone-d<sub>6</sub> (Sigma Aldrich, > 99.9 % d). All chemicals were used as received.

### **Reactor experiments**

The experiments were performed batchwise in a Parr autoclave of 50 mL. In each experiment, a borosilicate glass liner was filled with approximately 200 mg polyethylene, which was placed in the reactor. Then the reactor was purged with  $N_2$ , before pressurizing the vessel with the desired pressure  $O_2$  (Linde Gas) and  $N_2$  (Linde Gas). The reported pressures are measured at room temperature. Then, the reactor was heated to the desired temperature for a specified amount of time. The layer of PE at the bottom of the reactor was too thin to apply stirring. At the end, heating was stopped and the reactor was allowed to cool down to room temperature.

#### Product analysis and analytical methods

Gas chromatography (GC) was performed on a Thermo Scientific TraceGC 1300 instrument, equipped with a total ion chromatogram (TIC) and a flame ionization detector (FID). To prepare the crude product mixture obtained from the autoclave for injection it was esterified with a mixture of 6 mL acetyl chloride/methanol (1:20 v: v) following a literature procedure. [18] The mixture was stirred for 1 h at 50 °C. Thereafter, 5 mL *n*-heptane were added and both phases were separated using a separatory funnel. To both the methanol and n-heptane phase, respectively one drop of 4heptanone or cyclo-octane was added as internal standard. Prior to the injections the samples were filtered as a standard procedure to prevent the GC column from clogging The quantity of products in each phase was calculated separately and their yields were combined. The use of both phases was necessary to obtain reproducible results, because of the large variation in physical properties of the product mixture (e.g., C4 vs. C30). All products were assigned based on their mass spectrum (MS).

In-situ infrared (IR) spectroscopy experiments were performed on a PerkinElmer Frontier FTIR spectrometer, using a Linkam THMS600 microstage with CaF<sub>2</sub> windows (of 10 mm diameter and 1 mm thickness). The inlet and outlet were left open to the ambient. The sample consisted of a CaF2 plate with some PE grains. Timedependent experiments were performed by heating the sample with a rate of 60 °C/min to the desired temperature. When the polymer was molten, a spot with sufficient transmission was selected; for the experiments with catalyst a spot with approximately 70% PE and 30% catalyst was selected. Furthermore, an aperture size of 100 x 100  $\mu m$  was used to monitor the spectral changes. Arrived at the desired temperature, spectral collection was started. At the beginning of all experiments polymer flows as a result of melting were observed. During the experiment, the polymer continued to spread over the CaF<sub>2</sub> plate; as a consequence, different droplets of PE merge resulting in rearrangements of the polymer on the CaF<sub>2</sub> disk. In the obtained spectra these phenomena are reflected in small discontinuities in amount of reaction products observed.

Samples for the nuclear magnetic resonance (NMR) spectroscopy experiments were prepared by dissolving the complete crude reaction mixture ( $\sim$ 150–200 mg) in 0.5 mL of acetone-d<sub>6</sub>. All NMR experiments were performed at 25 °C on a Bruker Avance Neo 900 MHz spectrometer equipped with a Bruker 5 mm triple resonance (i. e.,  $^{1}$ H,  $^{13}$ C,  $^{15}$ N and  $^{2}$ H lock). CryoProbe with z-gradients in combination with a Bruker SampleCase cooled sample changer. The  $^{1}$ H -  $^{1}$ H total correlation spectroscopy (TOCSY) and heteronuclear multiple bond coherence (HMBC) spectra were recorded with a total of 2048 and 3072 data points in the direct dimension, respectively, 512 data points in the indirect dimension, 8 scans, a relaxation delay of 2 s, with an overall experimental time of 2 h and 30 min. The HSQC experiments were recorded with 3072 total data

points in the direct dimension, 1024 data points in the indirect dimension, 8 scans, a relaxation delay of 1.5 seconds, with an overall experimental time of 3 h and 45 min.

Combined thermogravimeterical analysis-mass spectrometry (TGA-MS) experiments were performed in a PerkinElmer TGA 8000 coupled to a Mass Spectrometer Hiden Analytical HPR-20 mass spectrometer. About 3 mg PE powder was loaded in a ceramic crucible. The product evolution and weight were monitored, using a temperature ramp of 5 °C/min. The experiments were performed in a  $O_2$ /Ar (20/80) atmosphere; Ar was used instead of  $N_2$ , because of the expected overlap with CO.

Differential scanning calorimetry (DSC) experiments were performed on a Discovery DSC instrument. For each experiment about 5 mg of the polymer was loaded in a DSC pan. For each sample, two heating/cooling cycles were performed with a heating ramp of  $10\,^{\circ}\text{C/min}$  and a cooling ramp of  $5\,^{\circ}\text{C/min}$ . The melting points  $(T_m)$  were derived from the first heating and the crystallization temperature  $(T_c)$  from the first cooling.

# Acknowledgements

The authors acknowledge Jochem Wijten and Ramon van Oord, both from the Inorganic Chemistry and Catalysis research group of Utrecht University (UU), for their technical support for the building of the experimental setup. We thank Hugo van Ingen (UU) and Andrei Gurinov (UU) from the NMR Spectroscopy research group for recording the NMR spectra. This work was supported by a joint funding through TNO/Brightsite and MCEC, a Netherlands Organization for Scientific Research (NWO) funded Gravitation program as well as by Advanced Research Center Chemical Building Blocks Consortium (ARC CBBC), which is co-founded and co-financed by NWO and the Netherlands Ministry of Economic Affairs and Climate Policy.

### Conflict of Interests

The authors declare no conflict of interest.

## Data Availability Statement

All data and python scripts utilized in the manuscript have been uploaded to the YODA repository and are available under https://doi.org/10.24416/UU01-5HD2P8.

**Keywords:** polyethylene  $\cdot$  chemical recycling  $\cdot$  di-carboxylic acids  $\cdot$  aerobic oxidation  $\cdot$  spectroscopy

- The Ellen MacArthur Foundation, The New Plastics Economy: Rethinking the Future of Plastic & Catalysing Action, 2013.
- [2] K. Ragaert, L. Delva, K. Van Geem, *Waste Manage*. **2017**, *69*, 24–58.
- [3] J. P. Lange, ACS Sustainable Chem. Eng. 2021, 9, 15722–15738.
  [4] I. Vollmer, M. J. F. Jenks, R. Mayorga González, F. Meirer, B. M.
- Weckhuysen, *Angew. Chem. Int. Ed.* **2021**, *60*, 16101–16108. [5] J. E. Remias, T. A. Pavlosky, A. Sen, *Acad. Sci. Paris* **2000**, *3*, 627–629.
- [6] A. K. P. Sullivan, A. Z. Werner, K. J. Ramirez, L. D. Ellis, J. Bussard, B. A. Black, D. G. Brandner, F. Bratti, B. L. Buss, X. Dong, S. J. Haugen, M. A.



- Ingraham, M. O. Konev, E. William, J. Miscall, I. Pardo, S. P. Woodworth, A. M. Guss, Y. Román, S. S. Stahl, *G. T. Beckham, Science* **2022**, *378*, 207–211.
- [7] K. E. Nicholas, Dibasic ester: A low risk, green organic solvent alternative, 2002, 238–253.
- [8] E. Bäckström, K. Odelius, M. Hakkarainen, ACS Sustainable Chem. Eng. 2019, 7, 11004–11013.
- [9] F. Gugumus, Polym. Degrad. Stab. 2002, 76, 329-340.
- [10] E. Chiellini, A. Corti, S. D'Antone, R. Baciu, Polym. Degrad. Stab. 2006, 91, 2739–2747.
- [11] J. D. Peterson, S. Vyazovkin, C. A. Wight, Macromol. Chem. Phys. 2001, 202, 775–784.
- [12] D. Briassoulis, A. Aristopoulou, M. Bonora, I. Verlodt, I. Biosyst. Eng. 2004, 88. 131–143.
- [13] U. W. Gedde, J. Viebke, H. Leijstrom, M. Ifwarson, Polym. Eng. Sci. 1994, 34, 1773–1787.
- [14] E. Bäckström, K. Odelius, M. Hakkarainen, Ind. Eng. Chem. Res. 2017, 56, 14814–14821.
- [15] L. R. Melby, Macromolecules 1978, 11, 50-56.
- [16] K. Pinsuwan, P. Opaprakasit, A. Petchsuk, L. Dubas, M. Opaprakasit, Polym. Degrad. Stab. 2023, 210, 110306.
- [17] A. Pifer, A. Sen, Angew. Chem. Int. Ed. 1998, 37, 3306-3308.
- [18] W. Partenheimer, Catal. Today 2003, 81, 117–135.
- [19] W. Partenheimer, US 6,958,373 B2, 2005.
- [20] J. Yun Yao, Y. Wen Wang, T. Muppaneni, R. Shrestha, J. Le Roy, G. D. Figuly, US 2019/0322833 A1, 2019.
- [21] E. Richaud, F. Farcas, P. Bartoloméo, B. Fayolle, L. Audouin, J. Verdu, Polym. Degrad. Stab. 2006, 91, 398–405.
- [22] R. K. Jensen, S. Korcek, L. R. Mahoney, M. Zinbo, J. Am. Chem. Soc. 1979, 101, 7574–7584.
- [23] R. K. Jensen, S. Korcek, M. Zinbo, J. Am. Chem. Soc. 1992, 114, 7742– 7748
- [24] H. N. Cheng, F. C. Schilling, F. A. Bovey, F. A. Macromolecules **1976**, *9*, 363–365.
- [25] S. M. Parke, J. C. Lopez, S. Cui, A. M. LaPointe, G. W. Coates, Angew. Chem. Int. Ed. 2023, 62, e202301927.
- [26] A. C. Schmidt, M. Hermsen, F. Rominger, R. Dehn, J. H. Teles, A. Schäfer, O. Trapp, T. Schaub, *Inorg. Chem.* 2017, 56, 1319–1332.
- [27] L. Chen, K. G. Mallollari, A. Uliana, D. Sanchez, Philip B. Messersmith, J. F. Hartwig, Chem 2021, 7, 137–145.

- [28] A. Bunescu, S. Lee, Q. Li, J. F. Hartwig, ACS Cent. Sci. 2017, 8, 895–903.
- 29] L. J. Missio, J. V. Comasseto, Tetrahedron: Asymmetry 2000, 11, 4609–4615.
- [30] R. Sang, P. Kucmierczyk, R Dühren, R. Razzaq, K. Dong, J. Liu, R Franke, R. Jackstell, M. Beller, Angew. Chem. 2019, 131, 14503–14511.
- [31] S. Tang, F. Seidel, K. Nozaki, Angew. Chem. Int. Ed. 2021, 60, 26506– 26510.
- [32] F. Gugumus, Polym. Degrad. Stab. 1999, 65, 5-13.
- [33] I. Yaremenko, V. A. Vil', D. V. Demchuk, A. O. Terent'ev, Beilstein J. Org. Chem. 2016, 12, 1647–1748.
- [34] N. Kosaka, T. Hiyama, K. Nozaki, Macromolecules 2004, 37, 4484–4487.
- [35] G. Socrates, Infrared and Raman Characteristic Group Frequencies. Tables and Charts, 3<sup>rd</sup> ed., John Wiley & Sons, New York, 2004, pp 115–154 and 259–281.
- [36] M. Salvalaggio, R. Bagatin, M. Fornaroli, S. Fanutti, S. Palmery, E. Battistel, Polym. Degrad. Stab. 2006, 91, 2775–2785.
- [37] M. Gardette, A. Perthue, J. L. Gardette, T. Janecska, E. Földes, B. Pukánszky, S. Therias, *Polym. Degrad. Stab.* 2013, 98, 2383–2390.
- [38] P. Bracco, L. Costa, M. P. Luda, N. Billingham, Polym. Degrad. Stab. 2018, 155, 67–83.
- [39] R. K. Jensen, S. Korcek, L. R. Mahoney, M. Zinbo, J. Am. Chem. Soc. 1981, 103, 1742–1749.
- [40] H. Togo, Advanced Free Radical Reactions for Organic Synthesis, Elsevier, 2004, pp 171–185.
- [41] W. Yan, G. Zhang, J. Wang, M. Liu, Y. Sun, Z. Zhou, W. Zhang, S. Zhang, X. Xu, J. Shen, X. Jin, Front. Chem. 2020, 8, 185.
- [42] L. Li, Y. Yao, N. Fu, Eur. J. Org. Chem. 2023, 26, e202300166.
- [43] J. Claydan, N. Greeves, S. Warren, *Organic Chemistry, 2th ed.*, Oxford University Press, **2012**, pp 961 and 977.
- [44] H. B. Tinker, J. Catal. 1970, 19, 237–244.
- [45] A. L. Perkel, S. G. Voronina, Russ. Chem. Bull. 2019, 68, 480–492.

Manuscript received: August 14, 2023 Revised manuscript received: November 26, 2023 Accepted manuscript online: November 27, 2023 Version of record online: December 13, 2023